fermentation

MDPI

Article

Upgrading Denitrification by Optimal Adsorption of SCFAs from Sludge Alkaline Fermentation Liquid by Acid-Modified Sepiolite

Saisai Su [1], Shuyun Ning [1], Shaobo Wu [1], Yanqing Duan [1,*], Yanjuan Gao [2] and Zhihong Liu [2,*]

[1] Department of Environmental and Safety Engineering, Taiyuan Institute of Technology, 31 Xinlan Road, Taiyuan 030008, China; susaisai_2004@163.com (S.S.); 2220690114@tit.edu.cn (S.N.); 2120600531@tit.edu.cn (S.W.)

[2] College of Environmental Science and Engineering, Taiyuan University of Technology, Taiyuan 030024, China; gaoyanjuan@tyut.edu.cn

* Correspondence: duanyanqing@tit.edu.cn (Y.D.); liuzhihong@tyut.edu.cn (Z.L.)

Abstract: Sludge alkaline fermentation liquid (AFL) is a potential carbon source for biological denitrification. However, its effectiveness is limited due to the presence of nutrients and heavy metals. In this study, acid-modified sepiolite (MSEP) was used to extract short-chain fatty acids (SCFAs) from AFL under optimized conditions and then with the prepared MSEP-AFL as a carbon source for denitrification. The optimal condition with an MSEP dosage of 1.96 g/L and pH 7.93 at 30 °C was obtained based on single-factor experiments and response surface methodology (RSM). Carbon balance revealed that 96.2% of the SCFAs, including 43.7% acetate and 23.5% propionic acid, was retained in the MSEP, demonstrating its high selectivity. The adsorption process followed the pseudo-second-order kinetic and Langmuir isothermal model, indicating dominant physical adsorption on the surface or in the fiber pores. This was further supported by the changes in the morphological features and surface properties of the MSEP. In the batch nitrate utilization experiments, the prepared MSEP-AFL was proven to be efficient as a carbon source, with a nitrate removal efficiency of 88.7% and a specific denitrification rate of 8.2 mg NOx-N/g VSS·h, which was 22% higher than that of the AFL. This was due to the establishment of a delicate "release–utilization" balance. These findings contribute to our understanding of the use of AFL for denitrification.

Keywords: alkaline fermentation liquid; carbon availability; denitrification; sepiolite; adsorption

Citation: Su, S.; Ning, S.; Wu, S.; Duan, Y.; Gao, Y.; Liu, Z. Upgrading Denitrification by Optimal Adsorption of SCFAs from Sludge Alkaline Fermentation Liquid by Acid-Modified Sepiolite. *Fermentation* **2024**, *10*, 476. https://doi.org/10.3390/fermentation10090476

Academic Editor: Alessio Siciliano

Received: 20 August 2024
Revised: 31 August 2024
Accepted: 3 September 2024
Published: 13 September 2024

1. Introduction

Biological nitrogen removal (BNR) is widely recognized as an essential task in wastewater treatment plants (WWTPs) to reduce effluent nitrogen discharge and alleviate the eutrophication of aquatic environments [1]. However, denitrification efficiency, as a crucial metric, is often hindered by an insufficient supply or utilization of organics, especially in WWTPs with influent wastewater with a low carbon-to-nitrogen ratio (C–N). This issue has become more severe with increasingly stricter discharge requirements. To address this problem, the addition of external carbon sources (ECSs) has been recognized as an essential measure to improve nitrogen removal. Examples of commonly used chemical agents include methanol, sodium acetate, and glucose. However, the high cost of purchasing these chemicals, as well as the need for accurate dosing and continuous monitoring, can be daunting [2]. Many studies have shown the effectiveness of waste-derived short-chain fatty acids (SCFAs) as a promising alternative for improving denitrification performance [3]. Mahmound discovered that the acidogenic fermentation liquid filtrates of various municipal and industrial wastes, such as food waste, whey powder, and bakery processing and kitchen wastes, had a higher potential for denitrification [4]. In order to reduce operational

costs, some industrial wastewater with high carbon content, such as soybean wastewater, has also been used for denitrification [5]. However, the widespread use of this ECS candidate was limited due to its significant heterogeneity and complex composition [6].

Waste activated sludge (WAS) is a readily available carbon source that is similar in composition to denitrification sludge [7]. Studies have shown that the SCFAs produced through the anaerobic fermentation of WAS, particularly alkaline fermentation liquid (AFL), were effective for denitrification on a pilot scale [8]. Acetate and propionate acids, the main components of SCFAs, have been found to be more efficient in removing nitrogen compared to glucose, methanol, and ethanol [9], and also resulted in lower emissions of N_2O [10]. Shao revealed that a nitrate removal rate of up to 96.4% could be obtained with sludge alkaline fermentation broth as a carbon source for denitrification [11]. Additionally, the potential benefits from sludge reduction and resource recovery were impressive, as reported by Zhang [12]. However, as a kind of liquid-phase carbon source, the dosage amount was difficult to be controlled due to its fast reaction speed and easy adsorption. This can result in higher effluent COD levels and require additional aeration energy to meet water quality standards. Meanwhile, accurately controlling the dosage amount and rate also incurs high operational costs and requires ancillary facilities such as control systems and batch pumps, placing a financial burden on WWTPs [13]. Furthermore, the nitrogen and phosphorus present in AFL were likely to increase nutrient removal loading in the wastewater line [14]. Other pollutants such as heavy metals and hazardous materials can harm denitrifying bacteria when AFL is directly used [15]. Therefore, it is important to develop technologies that can extract SCFAs from AFL, reducing the nutrient removal loading in mainstream wastewater and allowing for a more precise control of carbon source utilization for denitrification.

To date, several methods for extracting SCFAs have been studied, including calcium precipitation [16], solvent extraction [17], membrane purification [18], and the preparation of slow-release carbon sources, such as in situ SCFA-LDH synthesis [19]. A total of 96.42% of butyric acid and 94.40% of acetic acid from fermentation broths can be extracted by two-step salting-out extraction, as revealed by Li [20]. Various solvents such as alcohols, ethers, aliphatic hydrocarbons, and ketone have also been used for SCFA extraction, each with their own limitations [17]. While the calcium complexation of organic acids through the addition of Ca $(OH)_2$ or $CaCO_3$ combined with sulfuric acid release could result in high-purity acids, it is limited by the production of low-value calcium sulfate and high consumption due to the purchase of chemical agents [21]. Additionally, membrane technology has shown promise in SCFA extraction, but it has been hindered by the presence of other anions [7]. The in situ synthesis of layered double hydroxides with calcium addition was creatively proposed with extracted SCFAs as slow-release carbon sources [22], which established a subtle dynamic "release–utilization" balance for higher organic availability and denitrification efficiency [23]. Although the in situ synthesis process was affected by varied environmental factors and complex components of AFL, this approach expended the utilization of other porous materials in the upgrading of denitrification efficiency via improved carbon availability and utilization through SCFA extraction.

Sepiolite is a kind of low-cost magnesium phyllosilicate with a fibrous structure and microporous channels within the fiber axis, which gives it a higher sorption capacity than other clays due to its porous nature and large surface area. Due to its high adsorption efficiency, especially after modification, sepiolite has been used in various applications such as heavy metal adsorption [24], phosphorus removal [25], and stearic acid adsorption [26]. Its abundant reserves and low price made it possible to alleviate part of the financial burden in AFL production and adsorbent modification. However, the effect of sepiolite serving as an adsorbent of AFL is rarely studied. It is also not clear whether sepiolite can efficiently adsorb SCFAs and maintain a higher carbon source release capacity for denitrification.

The main purpose of this project was to investigate the adsorption performance and mechanism of MSEP on SCFA selection from AFL and its application in the denitrification process. The specific objectives were (1) to investigate the effects of initial AFL concentration,

MSEP dosage, pH value, and temperature on AFL adsorption efficiency and obtain the optimal adsorption condition using response surface methodology (RSM); (2) to explore the underlying adsorption mechanism through kinetic and isotherm studies as well as surface and structural feature analysis of MSEP using scanning electron microscope (SEM), Brunauer–Emmett-Teller (BET), X-ray diffractometer (XRD), and Fourier-transform infrared (FTIR) analyses; and (3) to evaluate the nitrate removal efficiency and carbon utilization when MSEP carried with AFL is used as a carbon source. This study aimed to find a more effective way to enhance denitrification efficiency by maximizing the extraction efficiency of SCFAs from AFL available for denitrifying bacteria.

2. Materials and Methods

2.1. Preparation of Modified Sepiolite and Acidogenic Fermentation Liquid

The RSEP was supplied by Xiangtan Shifeng Environmental Protection Technology Co., LTD, Hubei, China. After being washed with deionized water and dried for 24 h at 80 °C, the RSEP was modified with 4 mol/L hydrochloric acid (HCl) (solid–liquid mass ratio of 1:10) in a magnetic stirrer and heater system at 40 °C for 6 h [26]. After dumping the supernatant, the modified SEP (MSEP) samples were washed and filtered before drying in an oven at 110 °C for 16 h. The sludge for fermentation was collected from the secondary sedimentation tank in the Beijiao wastewater treatment plant in Shanxi, China. The sludge for denitrification was collected from the anoxic pond in the same WWTP and acclimated with 0.05% acetate for 48 h. Then, nitrogen was sparged for 10 min to flush out the extra oxygen in the sludge. After that, the sludge was washed several times with a phosphate buffer solution (PBS) to avoid any COD residue and adjusted to an MLVSS concentration of 4 g/L before use.

The AFL was obtained by batch mesophilic fermentation of municipal WAS in an anaerobic fermenter for 5 days on a lab scale. A thermal-alkalic pretreatment of the WAS was conducted to improve SCFA production with a pH value of 10 in an air bath oscillator at 80 °C for 2 h. The composition of the AFL was as follows: soluble chemical oxygen demand (SCOD) 4367 ± 84 mg/L, SCFA 2365 ± 107 mg COD/L, soluble proteins (SPr) 1356 ± 41 mg COD/L, and soluble carbohydrates (SCa) 454 ± 27 mg/L mg COD/L. The SCFAs were the sum of acetate (HAc, 1252 ± 41 mg COD/L), propionate acid (HPr, 268 ± 17 mg COD/L), iso-butyric acid (iso-HBu, 177 ± 13 mg COD/L), n-butyric acid (n-HBu, 200 ± 15 mg COD/L), iso-valecid (iso-HVa, 390 ± 11 mg COD/L), and n-valeric acid (n-HVa, 78 ± 6 mg COD/L).

2.2. Experimental Design of AFL Adsorption by RSEP

Batch-scale adsorption experiments were carried out in a series of 250 mL beakers on a magnetic stirrer with a heating function. Different AFL initial concentrations with dilution ratios of 1, 1.75, 2, and 5 were prepared to simulate AFL from thermal-alkalic pretreated sludge, AFL from non-pretreated sludge, AFL under natural fermentation conditions (20 °C, non-strict anaerobic fermentation), and SCFAs in the influent of typical WWTPs. The effect of the dosage amount of the MSEP (1.0, 1.5, 2.0, and 2.5 g/L) on the AFL adsorption was conducted when the pH value was 7.0 at 20 °C. In addition, the effect of environmental conditions on raw AFL adsorption performance including pH value (pH = 3, 5, 7, and 9) and reaction temperature (10, 20, 30, and 40 °C) was investigated with an MSEP dosage of 1 g/L. The supernatant was collected before and after adsorption to evaluate the adsorption efficiency (marked as η, %), which was calculated by the difference between the initial and final COD concentration divided by the initial COD. The collected samples were centrifuged and filtered to determine the SCOD concentration and compositions including SCa, SPr, and SCFAs.

Based on the adsorption performance of single factors, RSM in the software Design-Expert V. 13.0.1.0 was used to optimize the adsorption conditions. Three crucial factors, MSEP dosage (A), pH value (B), and temperature (C), were chosen as independent variables, with adsorption efficiency as the dependent variable. Based on the central composite design

(CCD), 17 experimental runs were conducted with the specific range and levels of the experiments listed in Table 1. The experiments were conducted in the same manner as the single factors. In addition to the COD measurement, the SCFA spectra under optimal conditions were measured including HAc, HPr, iso-HBu, n-HBu, iso-HVa, and n-HVa.

Table 1. Response surface design arrangement and experimental results.

Runs	Variables			η_{exp} (%)	η_{pre} (%)
	A	B	C		
1	2	6	40	87.3	91.7
2	1	9	25	82.7	87.2
3	1.5	6	25	81.2	84.5
4	1	6	40	82.4	85.9
5	1.5	9	10	81.7	85.5
6	2	9	25	85.2	89.5
7	1.5	6	10	78.6	77.9
8	1.5	3	40	57.6	58.0
9	1.5	3	25	47.2	48.0
10	1.5	3	10	44.1	45.9
11	2	6	25	83.4	82.7
12	2	6	25	79.7	80.3
13	1	6	10	76.4	78.5
14	2	3	25	50.2	50.1
15	1.5	9	40	91.3	93.9
16	1	3	25	48.7	48.4
17	2	6	10	78.9	80.4

A = MSEP dosage (g/L); B = pH value; C = temperature (°C); η_{exp} and η_{pre} = mean AFL adsorption efficiency based on experiments and model prediction, respectively (%).

2.3. Adsorption Mechanism Exploration

The adsorption kinetic can be used to predict the AFL adsorption rate via MSEP. In contrast, the adsorption isotherm model was used to describe the interactive behavior between the AFL and MSEP and to predict the adsorption capacity. This was beneficial for the exploration of the potential adsorption mechanism. In this study, the adsorption experimental data were modeled by two kinetic models, the pseudo-first-order (Equation (1)) and pseudo-second-order model (Equation (2)).

$$q_t = q_e\left(1 - e^{-k_1 t}\right) \tag{1}$$

$$\frac{t}{q_t} = \frac{1}{K_2 {q_e}^2} + \frac{1}{q_e}t \tag{2}$$

where k_1 is the rate constant of adsorption (1/min); q_e (mg/g) and q_t (mg/g) are the AFL amount at equilibrium and at time t (min), respectively; and k_2 (g/mg·min) is the rate constant of pseudo-second-order adsorption (1/min).

Two adsorption isotherm models were used, the Langmuir model (Equation (3)) and the Freundlich linear fitting model (Equation (4)).

$$\frac{C_e}{q_e} = \frac{C_e}{Q_m} + \frac{1}{Q_m K_L} \tag{3}$$

$$logq_e = logK_F + \frac{1}{n}logC_e \tag{4}$$

where q_e (mg/g) is the equilibrium adsorption amount of the AFL; c_e (mg/L) is the equilibrium concentration of the AFL; Q_m (mg/g) is the maximum adsorption capacity; and K_L represents the Langmuir constant, of which a larger value suggests a stronger affinity of the AFL and MSEP. K_F and n are the adsorption constants.

In addition, the MSEP under optimal conditions was collected at the end of the experiments to examine changes in its morphological characteristics, surface properties, and the distribution of functional groups, with the RSEP as the control. The morphological characteristics of the MSEP before and after adsorption were observed by SEM (SU8020, Hitachi Co., Tokyo, Japan). The BET surface area was determined using N_2 adsorption at −195.8 °C with a Quantachrome instrument (Autosorb-iQ, Quantachrome Instrument, USA). In addition, the crystalline phases of the sepiolite samples were obtained in Theta-2Theta configuration with step size of 0.02 and scan step of 1 s on an XRD with Cu-Kalpha radiation (PW1050, Philips, Newtheland). The FTIR spectrophotometry measurements were performed on an infrared spectrophotometer (Bruker TENSOR-27, Ettlingen, Germany) in the spectral range of 4000–400 cm^{-1} after being pressed to 1 mm KBr pellets.

2.4. Nitrate Utilization Experiments

To evaluate the denitrification capacity of the MSEP-AFL, nitrate utilization tests were performed with AFL as the control. A series of batch reactors with a working volume of 1 L was used for the tests. First, 10% of the denitrification seed sludge (with VSS adjusted to 4 g/L before use) was added in the reactors with the initial nitrate concentration adjusted to 50 ± 2 mg/L via a sodium nitrate stock solution (1000 mg/L). The ECS dosage was set as 230–250 mg SCOD/L based on the SCOD/NO_3-N of 5. The reactors were operated at room temperature for 6 h on a magnetic stirrer after sealing and blowing off the oxygen by nitrogen. Three parallels were conducted in each group. The samples were taken every 10 min for the first 1 h, every 30 min for the following 2 h, and every 60 min for the last 3 h. After centrifuging and filtering, the SCOD, NO_3-N, and NO_2-N were measured to evaluate the denitrification efficiency.

To evaluate the enhancement in the denitrification capacity of the MSEP-AFL, the specific denitrification rates (SDNR, k_N) were calculated as the linear portion of NO_x-N (calculated by the sum of NO_3^- and 0.6 NO_2^-) divided by the quantity of biomass [4].

$$\text{SDNR} = \frac{(NO_x - N_{initial}) - (NO_x - N_t)}{VSS \cdot t} [=] \frac{\text{mgNO}_x - \text{N}}{\text{gVSS} \cdot \text{h}} \quad (5)$$

where NO_x-$N_{initial}$ and NO_x-N_t are the NO_x-N concentration at the beginning and time "t" of the experiments (mg/L); VSS is the biomass amount (3.9 g VSS/L); and t is the reaction time (h).

2.5. Analytical Methods

All the regular indexes were analyzed according to standard methods (Chinese Standard Methods for the Examination of Water, 2002) [27]. SCOD was determined by the potassium permanganate oxidation method. SCa and SPr were determined by the phenol-sulfuric method and a special protein kit with glucose and bovine serum albumin as the standard substances, respectively. SCFA concentration and spectra were determined by gas chromatography (GC, 7890, Agilent, Santa Clara, CA, USA) with a flame ionization detector (FID). NO_3-N and NO_2-N concentrations were determined by the ultraviolet spectroscopy method.

3. Results and Discussion

3.1. Adsorption Performance of MSEP on SCFAs

3.1.1. Optimization of Adsorption Conditions of MSEP on SCFAs from AFL

Figure 1 illustrates the adsorption performance of the MSEP on the AFL under varied conditions. As shown in Figure 1A, with the dilution of the AFL, the adsorption efficiency decreased. When raw AFL was used (with the initial concentration of 2300 mg COD/L), it obtained the highest adsorption efficiency of 83.4%, 3.7% higher than the group with the half concentration of the raw AFL. Still, 57.2% COD could be obtained when the AFL was further diluted to 460 mg/L (equivalent to influent COD concentration), suggesting a higher extraction efficiency of the prepared MSEP. The MSEP dosage could also affect the

COD adsorption efficiency. As revealed, with the increase in the MSEP dosage from 1 g/L to 2 g/L, less COD was left in the raw AFL, with COD adsorption efficiency increased from 72.3% to 91.7% at room temperature with a neutral pH value. It seems that the acidic condition was unfavorable, with the lowest adsorption efficiency of 46.7% and 56.7% with pH values of 3 and 5, respectively. This dramatically rose to 82.3% and 89.2% at neutral and alkaline pH values. The increase in the reaction temperature intensified the interaction between the adsorbent and adsorbate, resulting in a climbing of the adsorption efficiency from 75.6% at 10 °C to 92.3% at 40 °C.

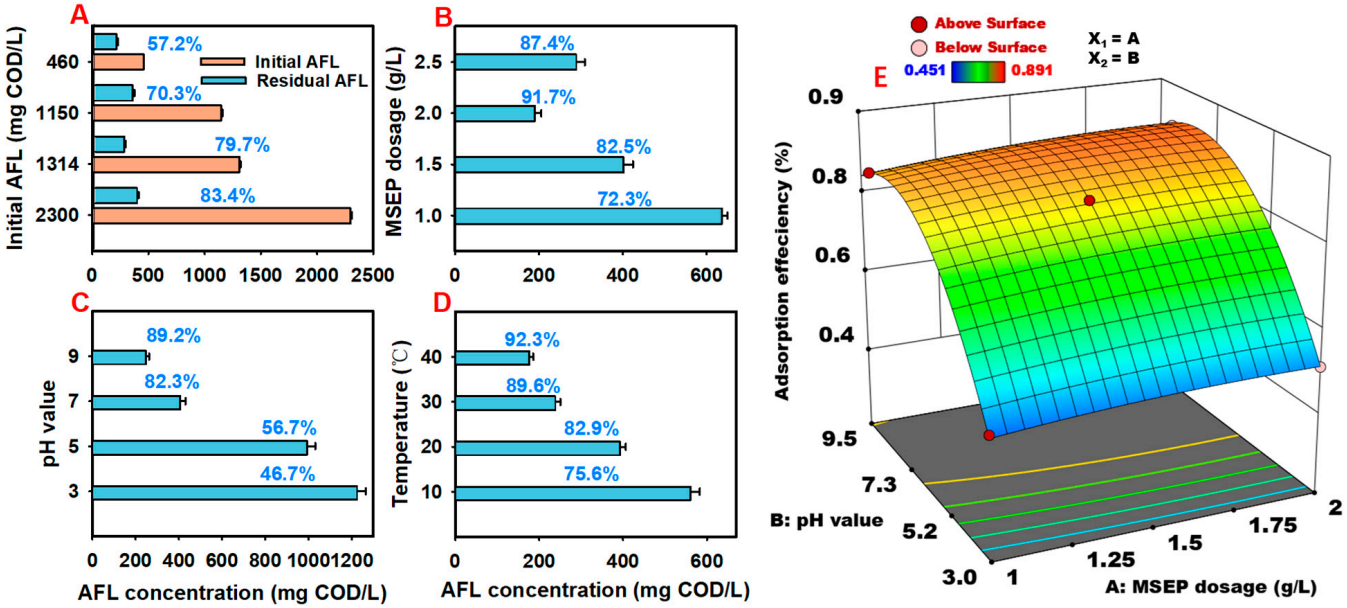

Figure 1. Optimization of AFL adsorption conditions: (**A**) the effect of initial AFL concentration; (**B**) the effect of MSEP dosage; (**C**) the effect of pH value; (**D**) the effect of temperature; (**E**) the response surface plot of the effect of MSEP dosage and pH value.

To evaluate the relationship of the crucial parameters on the AFL adsorption efficiency, the RSM method was applied to optimize the adsorption process via the development of the mathematical correlation between the selected parameters and AFL adsorption efficiency, as revealed by quadratic Equation (6):

$$\begin{aligned}\text{Adsorption efficiency } (\%) \; = \; & 0.8120 + 0.0143A + 0.0175B + 0.0649C + \\ & 0.0025AB + 0.0060AC + 0.0097BC - 0.0096A2 - 0.1354B2 + 0.0101C2\end{aligned} \quad (6)$$

The model coefficient (R^2 = 0.946) and probability *p*-value (<0.0001) indicated that the equation could provide a good explanation of the interaction effect between the parameters and the AFL adsorption efficiency. Based on Equation (2), the three-dimensional response surfaces and contour lines were presented (Figure 1E) with the optimum conditions of an MSEP dosage of 1.96 g/L and pH 7.93 at 30 °C with a predicted adsorption efficiency of 94.9%. As revealed by Table S1, pH value and temperature were the two significant factors, with an F-value of 1488.96 and 106.37, respectively ($p < 0.0001$). The lower lack of fit (sum of squares (SS) = 0.0012) compared to that of the model SS (0.3442) indicated the accuracy of the model fitting.

3.1.2. Composition of Sepiolite-Based Carbon Source under Optimal Conditions

To make clear whether the preferable carbon sources (mainly SCFAs) were adsorbed by the MSEP, a carbon balance before and after adsorption under optimal adsorption conditions is depicted in Figure 2. As demonstrated in Figure 2A, the highest adsorption efficiency of 92.3% was obtained under condition 1 (40 °C, initial AFL 2300 mg COD/L,

central pH value, and MSEP dosage 1.5 g/L). Of the total, 97.8% of the SCFAs in the raw AFL was adsorbed, also with 81.7% SPr and 95.4% SCa. More elaborately (Figure 2C), the SCFAs adsorbed on the MSEP included 43.7% HAc and 23.5% HPr with a lower proportion of other fatty acids, suggesting its capacity as an excellent carrier for an easily utilized carbon source. By contrast, with a moderate temperature of 20 °C and a higher MSEP dosage of 2 g/L, considerable SCFAs (96.2%) could also be conserved in the MSEP with an adsorption efficiency of 91.7%, although 6.3% less SCr was obtained. This high selectivity of SCFAs by the MSEP from the raw AFL could maximize the proportion of easily biodegradable organic carbons available for denitrification. Given that the sepiolite is easily available at a low cost, it is worthwhile to use more MSEP for the SCFA loss of less than 1%. Namely, compared to the higher energy input to raise the temperature to 40 °C (condition 2), it may be preferable to choose condition 1 as the optimal condition in terms of economic cost in actual applications (the samples and data were used for the following analysis and evaluation).

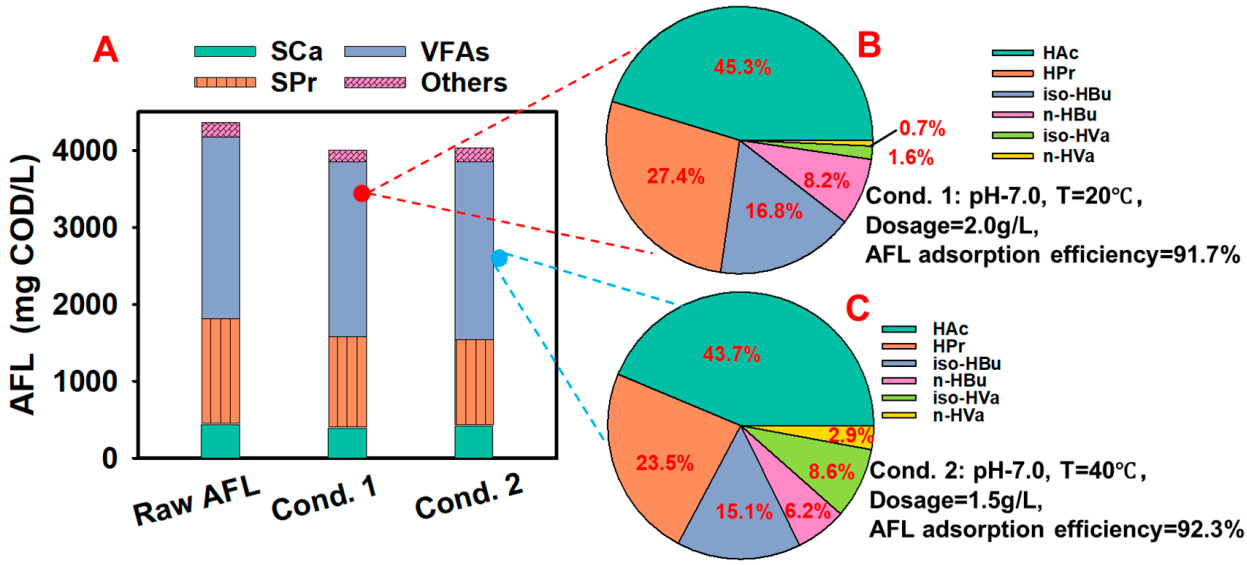

Figure 2. Carbon distribution of the adsorbed AFL (**A**) and the contained SCFA spectra under optimal adsorption conditions 1 (**B**) and conditions 2 (**C**).

3.2. Exploration of the Underlying Adsorption Mechanism by Kinetic Study and Property Characterization

3.2.1. Kinetic and Isotherm Study of the Adsorption Process

The kinetic fitting curve was used to understand the adsorption behavior by adsorption rate prediction, as shown by the line plots by ln ($q_e - q_t$) against t in Figure 3A. Compared with the pseudo-first-order model (with a correlation coefficient R^2 of 0.965), it seems that the pseudo-second-order model fit the experimental data better, with a higher R^2 of 0.988. This suggested that the adsorption process is in line with the universal rate law for a chemical reaction, namely, the adsorption rate depends on the availability of adsorption sites on the surface of the adsorbent rather than adsorbate concentration in the bulk solution. The obtained theoretical q_e of 1064.9 mg/g was more rational and closer to the experimental actual value of (1054.5 mg/g). The reaction rate constant k_2 was calculated as 1.74×10^{-4} g/(mg·min). This was similar to the results from Wu [28]. As revealed by Figure 3B, the Langmuir model (R^2 = 0.981) was more suitable than the Freudlich model (R^2 = 0.975) in describing the adsorption process. This means that the adsorption process was more likely to belong to monolayer absorption, with adsorption sites mainly on the surface or in the pores.

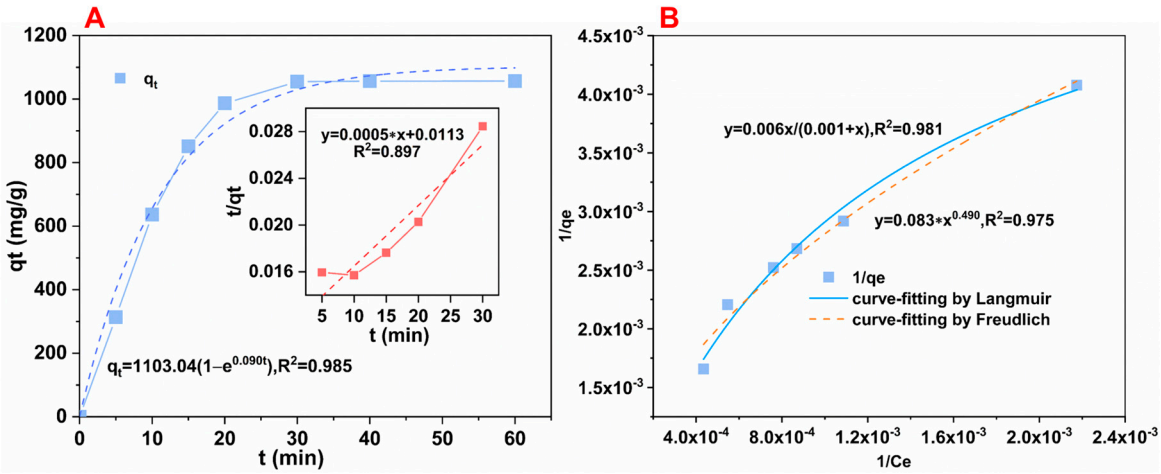

Figure 3. Curve fitting of the adsorption procedure: (**A**) kinetic fitting (the blue and red line for pseudo-first-order and pseudo-second-order model, respectively); (**B**) isotherm fitting (the blue and red line for Langmuir and Freudlich model, respectively).

3.2.2. Characterization of MSEP before and after Adsorption

Figure 4A illustrates the changes in the SEM images of the sepiolite. As revealed, the typical fibrous structure and microporous channels were observed, which have been reported to be made up of sheets of tetrahedral and octahedral oxides. After being modified by hydrochloric acid, the fiber structure was partially destroyed and became more dispersed than the RSEP, which might be more favorable for the adsorption of SCFAs into the pore structure of sepiolite. As confirmed by Figure 4(Ac), after adsorption, most of the surface of the MSEP has indeed been covered, suggesting the possibility that SCFAs and some other organics adhered to the surface and fiber pores of sepiolite. This was further verified by the changes in the surface area characteristics shown in the BET analysis, as shown in Table 2. The typical hysteresis loop indicated that the prepared MSEP is a typical mesoporous material. The results showed a 12% decrease in the BET surface area from 42.906 m^2/g to 37.747 m^2/g after adsorption. In addition, the average pore diameter increased from 3.035 nm to 3.407, and the pore volume decreased by 18% based on the BJH analysis. These changes confirmed the fact that the SCFAs and other organics like SCa and Spr were adsorbed on the surface or partially into the pore of the MSEP. The results were also consistent with the conclusion from thermodynamic studies.

The changes in the SEP could be partially confirmed by the XRD analysis. As revealed by Figure 4B, the difference between the characteristic peaks of the RSEP and MSEP was slight, such as sepiolite clay mineral (d = 7.31, 15.91, 27.86 Å), for instance. This suggested that the acid modification treatment did not impact the basic structure of the sepiolite. As another composition of sepiolite, the peak intensities of dolomite (23.71 Å) disappeared, indicating the leaching of Mg^{2+} and Ca^{2+} cations after acid modification. The slight changes between the MSEP before and after adsorption also manifested in that the adsorption was more likely on the surface. Figure 4C depicts the changes in the functional groups before and after adsorption. Typical characteristic peaks of SEP are shown at 472 cm^{-1} in addition to an average 1029 cm^{-1} for Si-O-Si bending and Si-O stretching vibration of the SEP tetrahedral layer, respectively. A deep bond at 676 cm^{-1} assigned to the bending vibration of Mg_3OH was also observed. The band at 800 cm^{-1} belonged to the C-O stretching vibrations, which was the featured group of carbonates (dolomite) in the sepiolite. The characteristic peaks assigned to various hydroxyl groups were also observed in a broad spectrum of 3000~4000 cm^{-1}. To be specific, the deep band at 3685 cm^{-1} belonged to the stretching vibrations of Mg_3OH placed in the inner structure of the SEP, while the broad band with an average peak wavenumber of 3435 cm^{-1} corresponded to H_2O in the RSEP and MSEP. Notably, the increased transmittance of these bonds after acid modification indicated drastic transformation of the sepiolite, such

as the leaching of magnesium cations, the loss of bound hydroxyl water coordinated to magnesium cations, and the disappearance of dolomite. What is more, the characteristic peaks of the carboxylate anion for asymmetric stretching vibrations and the -CH_3 group for the bending mode of the acetate anion appeared at 1631 cm^{-1} and 1355 cm^{-1}, respectively, indicating that the acetate was preferentially selected onto the surface of the MSEP.

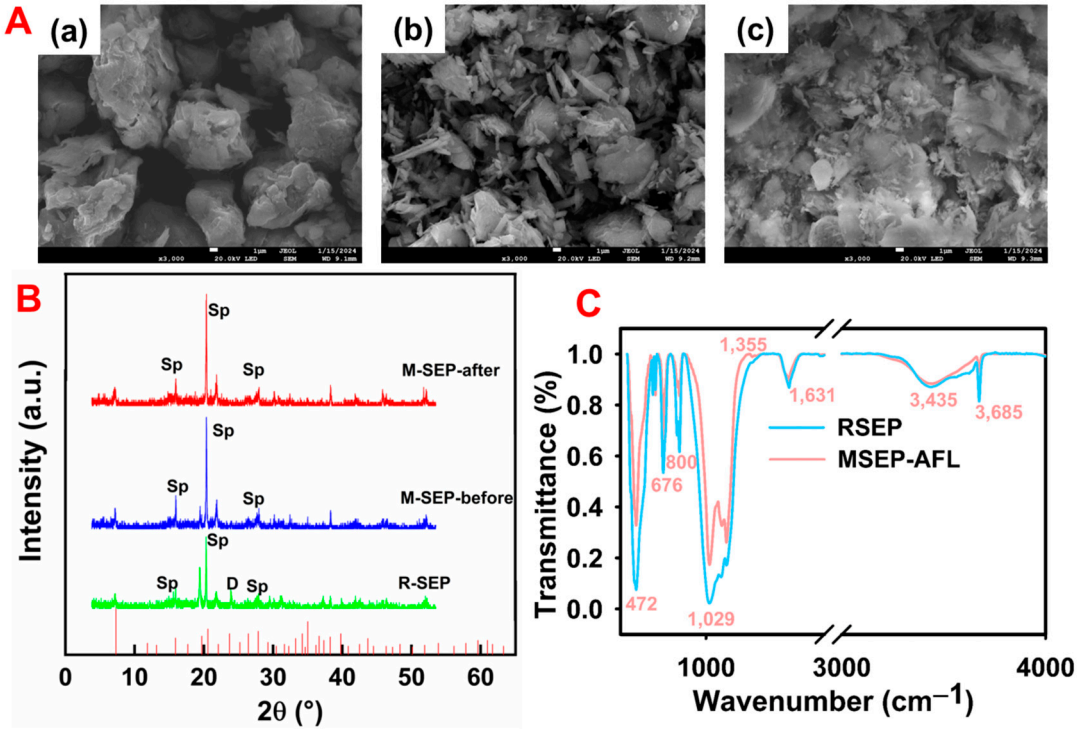

Figure 4. Changes in morphology and structure of MSEP: (**A**) SEM photographs of RSEP (**a**); MSEP before (**b**) and after (**c**) adsorption; (**B**) XRD patterns of RSEP and MSEP before and after adsorption, (Sp for sepiolite, D for dolomite); (**C**) FTIR spectra of MSEP before and after adsorption.

Table 2. Physical properties and adsorption capacities of MSEP before and after SCFA adsorption.

BET Surface Area (m^2/g)	Pore Volume (cm^3/g)	Average Pore Diameter (nm)	BJH Surface Area (m^2/g)
42.906	0.094	3.035	20.999
37.747	0.077	3.407	16.891

3.3. Denitrification Capacity of the MSEP-Based Carbon Source

The carbon sources were supplied based on a C–N ratio of 5, so the AFL and MSEP-AFL were diluted 19.4 times and 5.1 times, respectively. The composition of the carbon solution for the nitrate removal experiments is listed in Table S2. To reveal the denitrification performance, nitrate and nitrite were detected with reaction time, as revealed in Figure 5. As depicted, NO_3-N was removed within 6 h with a nitrate removal efficiency of 68.7% and 88.7% for the AFL and MSEP-AFL groups, respectively, indicating the occurrence of full denitrification. Specifically, three stages were observed in the linear regression curve [4]. It is worth noting that the concentration of NO_3-N dramatically decreased before 30 min with the AFL as the carbon source. This declining trend lasted until about 50 min when the MSEP-AFL was fed as the carbon source. The sharp decrease in NO_3-N was attributed to the utilization of easily biodegradable carbon sources (recorded as S_A), mainly HAc and HPr. As confirmed, HAc is preferable for denitrifying bacteria [29], with the largest SDNR of 0.0150 g NO_3-N/g VSS·d due to its simple pathway with only a single β-oxidation process [30]. The longer duration in the MSEP-AFL group was consistent with the high

proportion of HAc and HPr, leading to 66.9% nitrate removal efficiency at this stage (making up 75% of the total removal efficiency), 23.8% higher than that in the AFL group. The calculated SDNR was 6.3 mg NOx-N/g VSS·h and 8.2 mg NOx-N/g VSS·h for AFL and MSEP-AFL within one hour, respectively, as revealed by the liner regression ($R^2 > 0.98$). The higher value for the former was attributed to the high purity of HAc, which was slightly higher than the results from Shao with AFL as the carbon source [11]. With the depletion of NO_3-N, NO_2-N climbed due to the weak competition for electrons between NO_3-N reductase and NO_2-N reductase and then depleted immediately, converting to nitrogen. The second stage started with the declining trend slowing down when S_A was exhausted, and slowly biodegradable carbon sources (SFs) served as the carbon sources. Due to the low fraction of S_F, SPr for instance, the second phase was not as obvious in the MSEP-AFL group as that in AFL, making up 19.1% of the total removed nitrate. After the depletion of S_F, endogenous denitrification occurred with a slight decline in NO_3-N concentration.

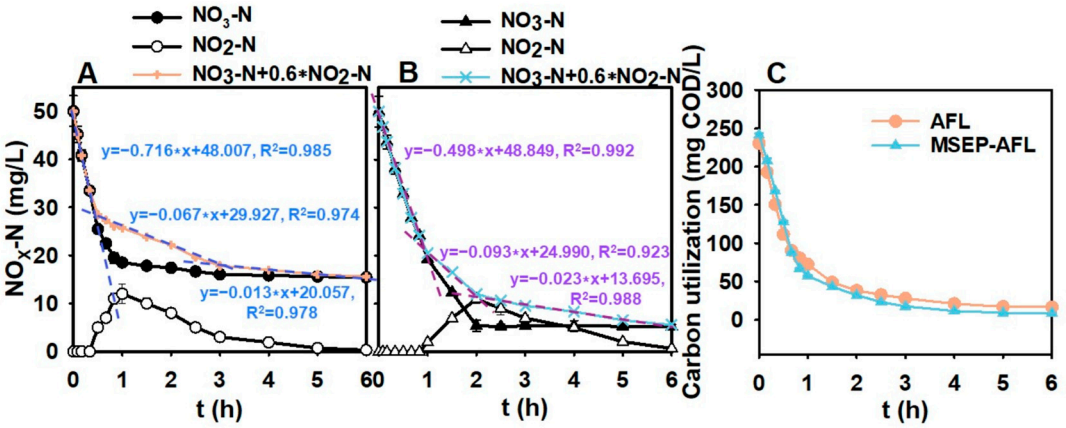

Figure 5. Performance of nitrate utilization of MSEP-AFL: (**A**) AFL and (**B**) MSEP-AFL NO_X-N changes and the curve fitting of the denitrification rate; (**C**) COD utilization of AFL and MSEP-AFL during the denitrification process.

As for the COD utilization (Figure 5C), 96.4% of the SCOD was degraded in the MSEP-AFL test within 6 h, corresponding to the continuous and steady decline in NO_3-N, as discussed before. The COD degradation efficiency in the AFL obtained 51.6% within 30 min and reached up to 92.8% at the end of the experiments, implying that the carbon source supplied was sufficient. This result was consistent with Mahmoud [4]. As reported, the slower COD consumption for the AFL and MSEP groups was due to multiple β-oxidation processes and more energy from denitrifying bacteria to remove the complicated organic carbon besides HBu and HVa, for instance. Note that the COD underwent a decline when the NO_3-N was stable. This might be due to the storage of intracellular carbon sources. As reported by Kujawa and Klapwijk, acetate shock was capable of stimulating microbial internal carbon source storage [31]. This was more significant in the MSEP group with a COD loss of about 3% since the high surface roughness was beneficial for the attachment of microorganisms with an endogenous denitrification function. This was similar to the results from Chang [32].

The denitrification potential, defined as the ratio of $\Delta COD–\Delta NO_3$-N (calculated by COD loss divided by the NO_3-N reduced amount), generally fell within the theoretical scale of 3–6 g COD/g NO_3-N [33]. For AFL, it was 4.7 mg COD/g NO_3-N, higher than the theoretical demand of 2.86 g COD/g N removed with acetate as the carbon source. This was due to the lower efficiency of energy capture by microorganisms (about 60% vs. 100% under the theoretical conditions) in the experimental conditions compared with the standard condition [4]. Meanwhile, the supplied COD was not only for denitrification but also for other heterotrophic bacteria. As reported by Guo [34], when there was a lower proportion of SCFAs in the supplied SCOD, the greater the carbon loss was for microorganism

growth. The MSEP-AFL obtained a higher value of 5.7 mg COD/g NO_3-N, which might be attributed to the improved purity of the supplied carbon as well as the slow-release pattern, which formed a dynamic "release–utilization" balance of the carbon source to make possible a higher nitrate removal efficiency and efficient carbon utilization, as reported by Jiang [23].

3.4. Underlying Mechanism and Potential Utilization of Sepiolite-Based Carbon Source in Promotion of Denitrification Efficiency

AFL has been recognized as a promising technology for enhancing denitrification efficiency. However, its widespread use has been limited by its rapid release, which might lead to carbon loss in internal storage due to excessive microorganism growth. To address this issue, a strategy was proposed to extract available carbon sources from AFL using mesoporous materials, such as sepiolite adsorption. This approach aims to improve denitrification efficiency by first significantly increasing the availability of carbon through the oriented selection adsorption of easily biodegradable carbon sources such as HAc and HPr. Secondly, the slow release of carbon sources helps to partially alleviate the excess levels of microorganisms caused by carbon shock. As a result, denitrification efficiency can be greatly improved by providing more available carbon sources for denitrifying bacteria while maintaining a dynamic "release–utilization" balance of these sources. Overall, this proposed strategy offers an updated approach for enhancing denitrification efficiency by simultaneously improving the availability of carbon sources and controlling their utilization.

Additionally, this strategy is expected to have economic and environmental benefits. Not only can it reduce the cost of sludge dewatering, but it can also save twice as much on carbon source supply by using an MSEP-AFL instead of a commercial ECS. This also eliminates the need for chemical agents and allows for the more efficient use of in situ produced SCFAs from WAS. Furthermore, the reduced use of fossil-derived agents and the reuse of sludge-embedded organics can help to reduce the risk of greenhouse gas emissions.

4. Conclusions

This study aimed to investigate the effectiveness of using MSEP to extract SCFAs from AFL and the impact of adding MSEP-AFL on nitrate removal and carbon utilization efficiency. The adsorption conditions were optimized through single-factor experiments (including initial AFL concentration, MSEP dosage, pH value, and temperature) and RSM based on a central composite design. A carbon balance analysis showed that the MSEP was able to adsorb over 90% of the SCFAs, with 43.7% HAc and 23.5% HPr, indicating its potential as a carrier for carbon sources. The adsorption process was well described by the pseudo-second-order kinetic model and Langmuir's isothermal adsorption model, suggesting that physical adsorption dominated on the surface or in the fiber pores. Furthermore, the SEM analysis showed a more dispersed fiber structure, the BET analysis revealed a reduced surface area, and the FTIR analysis showed a peak value for the functional group of HAc, all confirming that the SCFAs effectively adhered to the surface and fiber pores. Due to the high selection of SCFAs on the surface of the MSEP, the use of the MSEP-AFL for denitrification resulted in a high nitrate removal efficiency of 88.7% with a k_N of 8.2 mg NOx-N/g VSS·h, which was attributed to improved carbon availability and a subtle balance of the "release–utilization" of the carbon source. In conclusion, the proposed strategy of optimizing SCFA adsorption from AFL to improve carbon availability and establishing a balanced pattern of carbon "release–utilization" with MSEP-AFL as the carbon source showed promise in upgrading denitrification performance with high nitrate removal and efficient carbon utilization simultaneously.

Supplementary Materials: The following supporting information can be downloaded at https://www.mdpi.com/article/10.3390/fermentation10090476/s1, Table S1: ANOVA for the quadratic model fitted for AFL adsorption by MSEP; Table S2: The composition and SCFA spectra of diluted AFL and MSEP-AFL for denitrification.

Author Contributions: Conceptualization, Y.D.; methodology, S.S. and S.N.; software, S.N. and S.W.; validation, S.S., S.N. and Y.G.; formal analysis, S.S. and Y.G.; investigation, S.S.; resources, Y.D.; data curation, Y.G. and S.W.; writing—original draft preparation, S.S.; writing—review and editing, Y.D. and Z.L.; visualization, Y.G.; supervision, Z.L.; project administration, Y.D. and Z.L.; funding acquisition, Y.D. and Z.L. All authors have read and agreed to the published version of the manuscript.

Funding: This research was supported by the National Natural Science Foundation of China (NSFC, Nos.52100155), the China Postdoctoral Science Foundation (Nos. 2022M722007), the Fundamental Research Program of Shanxi Province (20210302124347, 20210302124133, and 202203021222280), and the Scientific and Technological Innovation Program of Higher Education Institutions in Shanxi (2022L549).

Data Availability Statement: The original data will be made available upon request.

Conflicts of Interest: The authors declare no conflicts of interest.

References

1. Yu, C.; Huang, X.; Chen, H.; Godfray, H.C.J.; Wright, J.S.; Hall, J.W.; Gong, P.; Ni, S.; Qiao, S.; Huang, G.; et al. Managing nitrogen to restore water quality in China. *Nature* **2019**, *567*, 516–520. [CrossRef] [PubMed]
2. Ding, H.; Tang, M.; Huang, Q.; Yang, P.; Liu, Z.; Bi, X.; Nair, A.; Wang, X. Soft sensor enabled real-time chemical dosing control systems for wastewater treatment: From hybrid model to full-scale application. *J. Water Process Eng.* **2024**, *63*, 105431. [CrossRef]
3. Ahmed, S.M.; Rind, S.; Rani, K. Systematic review: External carbon source for biological denitrification for wastewater. *Biotechnol. Bioeng.* **2023**, *120*, 642–658. [CrossRef] [PubMed]
4. Mahmoud, A.; Hamza, R.A.; Elbeshbishy, E. Enhancement of denitrification efficiency using municipal and industrial waste fermentation liquids as external carbon sources. *Sci. Total Environ.* **2022**, *816*, 151578. [CrossRef] [PubMed]
5. Xue, Z.; Wang, C.; Cao, J.; Luo, J.; Feng, Q.; Fang, F.; Li, C.; Zhang, Q. An alternative carbon source withdrawn from anaerobic fermentation of soybean wastewater to improve the deep denitrification of tail water. *Biochem. Eng. J.* **2018**, *132*, 217–224. [CrossRef]
6. Fu, X.; Hou, R.; Yang, P.; Qian, S.; Feng, Z.; Chen, Z.; Wang, F.; Yuan, R.; Chen, H.; Zhou, B. Application of external carbon source in heterotrophic denitrification of domestic sewage: A review. *Sci. Total Environ.* **2022**, *817*, 153061. [CrossRef]
7. Liu, W.; Yang, H.; Ye, J.; Luo, J.; Li, Y.-Y.; Liu, J. Short-chain fatty acids recovery from sewage sludge via acidogenic fermentation as a carbon source for denitrification: A review. *Bioresour. Technol.* **2020**, *311*, 123446. [CrossRef]
8. Zhang, F.; Chen, Y.; Zhao, F.; Yuan, P.; Lu, M.; Qin, K.; Qin, F.; Fu, S.; Guo, R.; Feng, Q. Use of magnetic powder to effectively improve the denitrification employing the activated sludge fermentation liquid as carbon source. *J. Environ. Manag.* **2023**, *348*, 119049. [CrossRef]
9. Xu, Z.; Dai, X.; Chai, X. Effect of different carbon sources on denitrification performance, microbial community structure and denitrification genes. *Sci. Total Environ.* **2018**, *634*, 195–204. [CrossRef]
10. Chen, H.; Wang, D.; Li, X.; Yang, Q.; Zeng, G. Enhancement of post-anoxic denitrification for biological nutrient removal: Effect of different carbon sources. *Environ. Sci. Pollut. Res.* **2015**, *22*, 5887–5894. [CrossRef]
11. Shao, M.; Guo, L.; She, Z.; Gao, M.; Zhao, Y.; Sun, M.; Guo, Y. Enhancing denitrification efficiency for nitrogen removal using waste sludge alkaline fermentation liquid as external carbon source. *Environ. Sci. Pollut. Res.* **2019**, *26*, 4633–4644. [CrossRef] [PubMed]
12. Zhang, W.; Xiao, B.; Li, Y.; Liu, Y.; Guo, X. Effects of return sludge alkaline treatment on sludge reduction in laboratory-scale anaerobic–anoxic–oxic process. *J. Biotechnol.* **2018**, *285*, 1–5. [CrossRef] [PubMed]
13. Qi, W.; Taherzadeh, M.J.; Ruan, Y.; Deng, Y.; Chen, J.-S.; Lu, H.-F.; Xu, X.-Y. Denitrification performance and microbial communities of solid-phase denitrifying reactors using poly (butylene succinate)/bamboo powder composite. *Bioresource Technol.* **2020**, *305*, 123033. [CrossRef] [PubMed]
14. Kılıç, M.; Yılmaz, T.; Partal, R.; Şık, E.; Doğan, Ö.; Kitis, M.; Sahinkaya, E. Nutrient recovery from anaerobic digester supernatant using a fluidized-bed reactor. *J. Water Process Eng.* **2023**, *54*, 103950. [CrossRef]
15. Lu, L.; Chen, C.; Ke, T.; Wang, M.; Sima, M.; Huang, S. Long-term metal pollution shifts microbial functional profiles of nitrification and denitrification in agricultural soils. *Sci. Total Environ.* **2022**, *830*, 154732. [CrossRef]
16. Li, Q.-Z.; Jiang, X.-L.; Feng, X.-J.; Wang, J.-M.; Sun, C.; Zhang, H.-B.; Xian, M.; Liu, H.-Z. Recovery Processes of Organic Acids from Fermentation Broths in the Biomass-Based Industry. *J. Microbiol. Biotechnol.* **2016**, *26*, 1–8. [CrossRef]
17. Bekatorou, A.; Dima, A.; Tsafrakidou, P.; Boura, K.; Lappa, K.; Kandylis, P.; Pissaridi, K.; Kanellaki, M.; Koutinas, A.A. Downstream extraction process development for recovery of organic acids from a fermentation broth. *Bioresour. Technol.* **2016**, *220*, 34–37. [CrossRef]
18. Aydin, S.; Yesil, H.; Tugtas, A.E. Recovery of mixed volatile fatty acids from anaerobically fermented organic wastes by vapor permeation membrane contactors. *Bioresour. Technol.* **2018**, *250*, 548–555. [CrossRef]
19. Sheng, L.; Ma, X.; Pan, F.; Liu, J.; Li, Y.-Y. Calcium peroxide pretreatment of waste activated sludge for enhancement of short chain fatty acids extraction from fermentation liquid by layered double hydroxides. *J. Clean. Prod.* **2020**, *246*, 119067. [CrossRef]

20. Li, Z.; Yan, L.; Zhou, J.; Wang, X.; Sun, Y.; Xiu, Z.-L. Two-step salting-out extraction of 1,3-propanediol, butyric acid and acetic acid from fermentation broths. *Sep. Purif. Technol.* **2019**, *209*, 246–253. [CrossRef]
21. Bhatia, S.K.; Yang, Y.-H. Microbial production of volatile fatty acids: Current status and future perspectives. *Rev. Environ. Sci. Biotechnol.* **2017**, *16*, 327–345. [CrossRef]
22. Sheng, L.; Liu, J.; Zhang, C.; Zou, L.; Li, Y.-Y.; Xu, Z.P. Pretreating anaerobic fermentation liquid with calcium addition to improve short chain fatty acids extraction via in situ synthesis of layered double hydroxides. *Bioresour. Technol.* **2019**, *271*, 190–195. [CrossRef] [PubMed]
23. Jiang, L.; Liu, J.; Zhang, C.; Duan, T.; Li, Y.; Zou, L.; Qian, G. Synthesis of Layered Double Hydroxides with Fermentation Liquid of Organic Waste To Extract Short-Chain Fatty Acids as a Biodenitrification Carbon Source. *ACS Sustain. Chem. Eng.* **2017**, *5*, 9095–9101. [CrossRef]
24. Wei, S.; Wang, L.; Wu, Y.; Liu, H. Study on removal of copper ions from aqueous phase by modified sepiolite flocs method. *Environ. Sci. Pollut. Res.* **2022**, *29*, 73492–73503. [CrossRef] [PubMed]
25. Gao, P.; Zhang, C. Study on Phosphorus Removal Pathway in Constructed Wetlands with Thermally Modified Sepiolite. *Sustainability* **2022**, *14*, 12535. [CrossRef]
26. Yan, W.-T.; Ye, W.-B.; Du, J.; Hong, Y. Improvement of acid modification and its effect on the adsorption of stearic acid into sepiolite. *J. Therm. Anal. Calorim.* **2021**, *147*, 3025–3032. [CrossRef]
27. EPA of China. *Water and Wastewater Monitoring Analysis Method*, 4th ed.; Chinese Environment Science Publisher: Beijing, China, 2002.
28. Wu, J.; Wang, Y.; Wu, Z.; Gao, Y.; Li, X. Adsorption properties and mechanism of sepiolite modified by anionic and cationic surfactants on oxytetracycline from aqueous solutions. *Sci. Total Environ.* **2020**, *708*, 134409. [CrossRef]
29. Sapmaz, T.; Manafi, R.; Mahboubi, A.; Lorick, D.; Koseoglu-Imer, D.Y.; Taherzadeh, M.J. Potential of food waste-derived volatile fatty acids as alternative carbon source for denitrifying moving bed biofilm reactors. *Bioresour. Technol.* **2022**, *364*, 128046. [CrossRef]
30. Elefsiniotis, P.; Wareham, D.G. Utilization patterns of volatile fatty acids in the denitrification reaction. *Enzym. Microb. Technol.* **2007**, *41*, 92–97. [CrossRef]
31. Kujawa, K.; Klapwijk, B. A method to estimate denitrification potential for predenitrification systems using NUR batch test. *Water Res.* **1999**, *33*, 2291–2300. [CrossRef]
32. Chang, M.; Fan, F.; Zhang, K.; Wu, Z.; Zhu, T.; Wang, Y. Denitrification performance and mechanism of a novel sulfur-based fiber carrier fixed-bed reactor: Co-existence of sulfur-based autotrophic denitrification and endogenous denitrification. *J. Water Process Eng.* **2023**, *53*, 103618. [CrossRef]
33. Chen, H.; Ye, Q.; Wang, X.; Sheng, J.; Yu, X.; Zhao, S.; Zou, X.; Zhang, W.; Xue, G. Applying sludge hydrolysate as a carbon source for biological denitrification after composition optimization via red soil filtration. *Water Res.* **2023**, *249*, 120909. [CrossRef] [PubMed]
34. Guo, Y.; Guo, L.; Sun, M.; Zhao, Y.; Gao, M.; She, Z. Effects of hydraulic retention time (HRT) on denitrification using waste activated sludge thermal hydrolysis liquid and acidogenic liquid as carbon sources. *Bioresour. Technol.* **2017**, *224*, 147–156. [CrossRef] [PubMed]